

ORIGINAL ARTICLE

# Viral vector-based improvement of optic nerve regeneration: characterization of individual axons' growth patterns and synaptogenesis in a visual target

BJ Yungher<sup>1</sup>, X Luo<sup>1</sup>, Y Salgueiro<sup>1</sup>, MG Blackmore<sup>2</sup> and KK Park<sup>1</sup>

Lack of axon growth ability in the central nervous system poses a major barrier to achieving functional connectivity after injury. Thus, a non-transgenic regenerative approach to reinnervating targets has important implications in clinical and research settings. Previous studies using knockout (KO) mice have demonstrated long-distance axon regeneration. Using an optic nerve injury model, here we evaluate the efficacy of viral, RNA interference (RNAi) and pharmacological approaches that target the phosphatase and tensin homolog (PTEN) and signal transducer and activator of transcription-3 pathways to improve long-distance axon regeneration in wild-type mice. Our data show that adeno-associated virus (AAV) expressing short hairpin RNA (shRNA) against PTEN (shPTEN) enhances retinal ganglion cell axon regeneration after crush injury. However, compared with the previous data in PTEN KO mice, AAV-shRNA results in a lesser degree of regeneration, likely due to incomplete gene silencing inherent to RNAi. In comparison, an extensive enhancement in regeneration is seen when AAV-shPTEN is coupled to AAV encoding ciliary neurotrophic factor (CNTF) and to a cyclic adenosine monophosphate (cAMP) analog, allowing axons to travel long distances and reach their target. We apply whole-tissue imaging that facilitates three-dimensional visualization of single regenerating axons and document heterogeneous terminal patterns in the targets. This shows that some axonal populations generate extensive arbors and make synapses with the target neurons. Collectively, we show a combinatorial viral RNAi and pharmacological strategy that improves long-distance regeneration in wild-type animals and provide single fiber projection data that indicates a degree of preservation of target recognition.

*Gene Therapy* (2015) 22, 811–821; doi:10.1038/gt.2015.51

## INTRODUCTION

Following injury, axons in the adult central nervous system generally fail to regenerate long distances and reinnervate their target. Using optic nerve injury and conditional knockout (KO) mice, we and others have previously demonstrated that deleting phosphatase and tensin homolog (PTEN) and suppressor of cytokine signaling 3 (SOCS3) in adult retinal ganglion cells (RGCs) allows long-distance optic nerve regeneration and target reinnervation to some degree.<sup>1–3</sup> Moreover, it was reported that PTEN KO combined with zymosan and cAMP analog induces long-distance regeneration and partial recovery of visual functions,<sup>4</sup> providing a framework for developing reparative therapy. However, whether non-transgenic approaches that modulate PTEN alone or with other growth-regulating factors can promote a similar level of RGC axon regeneration in wild-type animals has not been directly addressed. Adeno-associated virus (AAV) lacks significant pathogenicity and has been used safely in clinical trials for a number of ocular and non-ocular diseases.<sup>5</sup> Therefore, the first aim of this present study was to evaluate whether AAV vectors that incorporate RNA interference (RNAi) can suppress endogenous PTEN in adult RGCs and promote RGC axon regeneration in the adult mouse. Next, we examined whether combined viral RNAi and pharmacotherapy approaches that modulate PTEN and other growth promoters will further improve long-distance regeneration of axons to their brain targets.

On arriving at the final targets, the growth cones of long projecting axons switch from an extension program to one that facilitates target recognition and reconnection. One key feature during this process is the formation of axon arbors that facilitates connection with their proper target neurons. To visualize single axon and their entire arbors and to unequivocally assess axon terminals, several studies in model organisms including zebrafish have used single-cell labeling and whole-tissue imaging.<sup>6,7</sup> However, such techniques have not yet been established for the study of axon targeting in mammals. In our previous studies, we have described the use of optical clearance and whole-tissue imaging to assess RGC axon regeneration *in vivo*. In this present study, we expand the application of these imaging techniques, establish single axon visualization and determine terminal morphology of regenerating axons within a visual target in mice.

## RESULTS

Evaluation of AAV2-shRNA-mediated PTEN knockdown and RGC axon regeneration

Here we sought to examine the degree of RGC axon regeneration after AAV-shRNA-mediated PTEN knockdown. To this end, we first tested a shRNA strategy, using the RNA pol II vectors that is based on the primary transcript for the miR-155 microRNA, designated SIBR.<sup>8</sup> In a SIBR vector, shRNA is located in an intron and flanked

<sup>1</sup>Miami Project to Cure Paralysis, Department of Neurosurgery, University of Miami, Miller School of Medicine, Miami, FL, USA and <sup>2</sup>Department of Biomedical Sciences, Marquette University, Milwaukee, WI, USA. Correspondence: Dr KK Park, Miami Project to Cure Paralysis, Department of Neurosurgery, University of Miami, Miller School of Medicine, 1094 NW 14th Ter. RM 4-20, Miami, 33136 FL, USA.

E-mail: kpark@med.miami.edu

Received 5 February 2015; revised 10 April 2015; accepted 5 May 2015; accepted article preview online 25 May 2015; advance online publication, 18 June 2015

by sequences derived from mir155, an endogenous intronic shRNA. This design allows a single primary transcript to produce shRNA from intronic sequences, as well as an intact exon that encodes an enhanced green fluorescent protein (EGFP) reporter (Figure 1a). Furthermore, this design allows insertion of four separate shRNA sequences, concatenated in a single plasmid, each targeting a different region of PTEN (referred hereafter as 'shPTEN4'), thereby increasing the probability of effectively silencing the gene of interest. Alternatively, we used a previously tested PTEN targeting sequence<sup>9,10</sup> shown to be highly specific to PTEN (referred hereafter as shPTEN1).<sup>10</sup> Since AAV serotype 2 has been shown to effectively transduce postmitotic neurons including the RGCs,<sup>11</sup> these plasmids were then used to produce AAV serotype 2 (AAV-shPTEN4 or shPTEN1). To evaluate the knock-down efficiency of PTEN, we initially incubated rat cortical neurons with either AAV-anti-luciferase-EGFP (AAV-EGFP) or AAV-shPTEN4.

Seven days after treatment AAV-shPTEN4 markedly suppresses the endogenous expression of PTEN as shown by immunocytochemistry (Figure 1b;  $n=2$  biological replicates). To evaluate the gene knockdown efficiency in mouse RGCs, we injected AAV-shPTEN4 into the vitreous body of young adult C57BL/6 mouse eyes. In cross-section immunohistochemistry performed 2 weeks after injection, transduced RGCs show a significant reduction of PTEN expression compared with control RGCs transduced with AAV-EGFP (Figure 1c). Flat-mounted retinæ show over 90% transduction of RGCs by the AAV vector (Figure 1d;  $n=4$ ). Quantification using western blot in cortical neurons (Figures 1e and f) and PTEN intensity analysis in retina sections (Figure 1g), we observe about 70% reduction in PTEN level after AAV-shPTEN4. Consistent with the previous study,<sup>9,10</sup> AAV-shPTEN containing a single targeting sequence (AAV-shPTEN1) led to ~70% reduction in PTEN expression in adult RGCs (data not shown). As an initial

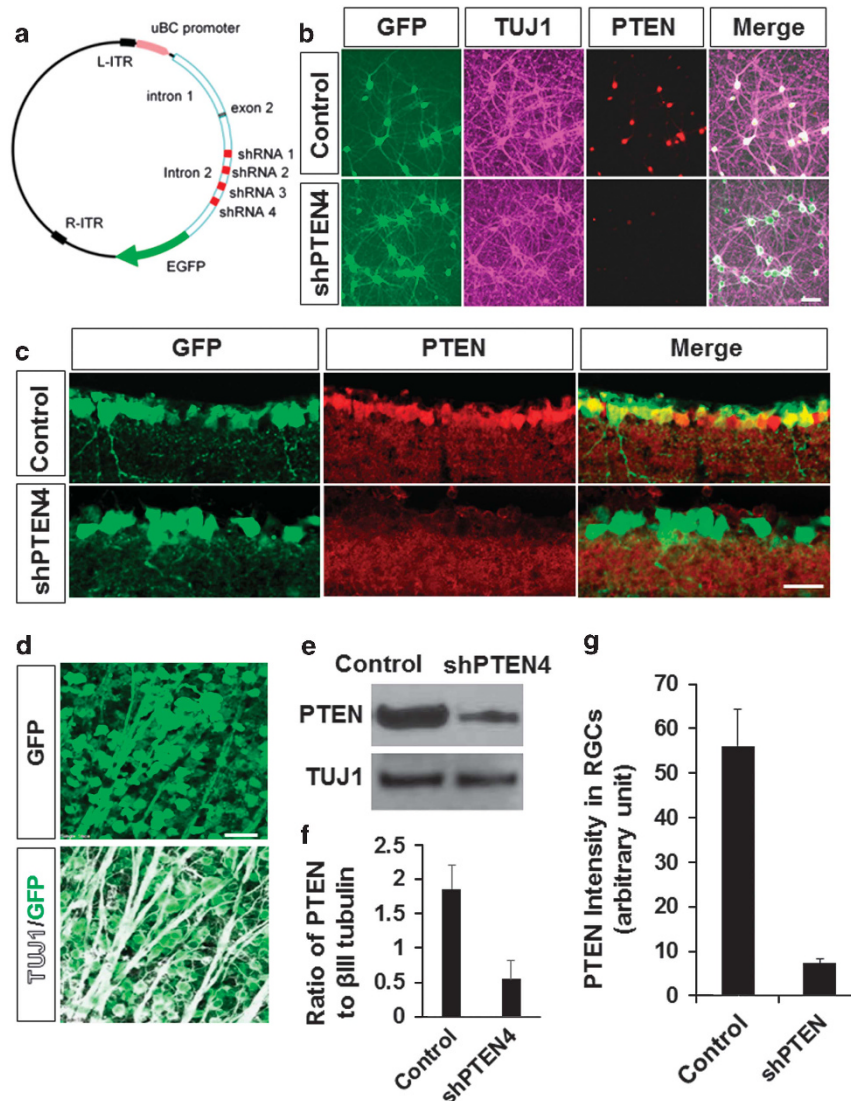


**Figure 1.** AAV-shRNA mediated suppression of PTEN. (a) A map of AAV2-shPTEN4 construct. Control and shPTEN constructs contain EGFP reporter. (b) Immunocytochemistry showing expression of GFP, PTEN and  $\beta$ III tubulin (TUJ1) in cultured cortical neurons incubated with either AAV-anti-luciferase-EGFP (control) or AAV-RNA against PTEN (AAV-shPTEN4) for 7 days. These are representative micrographs from two separate experiments. (c) Retina sections following control AAV2-EGFP (EGFP) or AAV2-shPTEN4 injection show PTEN knockdown in ganglion cell layer. (d) Flat-mounted retina 2 weeks following intravitreal injection of AAV2-shPTEN4, stained with antibodies against GFP and TUJ1 shows >90% transduction efficiency in RGCs. (e) Western blot of protein lysates extracted from cultured cortical neurons showing PTEN level at 7 days after the addition of AAV-shPTEN4 or AAV-EGFP. (f) Quantification of PTEN level from the western blot. Values are represented as ratio of PTEN to  $\beta$ III-tubulin ( $n=3$  biological replicates). (g) Quantification of PTEN expression in RGCs in retina sections, measured by ImageJ densitometry method. Intensity unit is an arbitrary value. Error bars, s.e.m. Scale bars, 20  $\mu$ m.

test to examine the effect of PTEN knockdown on RGC axon regeneration, we injected AAV-shPTEN4, AAV-shPTEN1 or AAV-EGFP 2 weeks before an optic nerve crush. Anterograde labeling of regenerating axons by cholera toxin  $\beta$ -subunit (CTB) injection occurred 2 days before euthanizing the mice. As expected, we observed significant increases in the number of axons growing beyond the lesion site in mice receiving either AAV-shPTEN4 (sixfold increase) or AAV-shPTEN1 (fourfold increase) compared with AAV-EGFP treatment at 0.2 mm from the lesion 4 weeks after injury (Figures 2a and b;  $n=5$ /group). We noticed, however, that the degree of regeneration in the AAV-shPTEN animals is less extensive than that of the PTEN KO mice (that is, PTEN<sup>f/f</sup> mice

subjected to AAV-Cre injection).<sup>1</sup> At 4 mm distal to the lesion (that is, near the chiasm), we did not observe regenerating axons in the AAV-shPTEN animals. On the other hand, more than 20 axons per one optic nerve section were seen at this distance in the PTEN KO animals treated with AAV-Cre.<sup>1</sup> Since we have previously shown that the level of axotomy-induced cell death is reduced by PTEN deletion in RGCs,<sup>1</sup> we also assessed whether AAV-mediated PTEN knockdown will similarly enhance RGC survival. By using an antibody against  $\beta$ III tubulin (TUJ1) to immunostain viable RGCs, we observed that AAV-shPTEN4 treatment results in a twofold increase in RGC survival rates compared with control mice (Figures 2c and d). Unlike the difference seen in regeneration rate, this

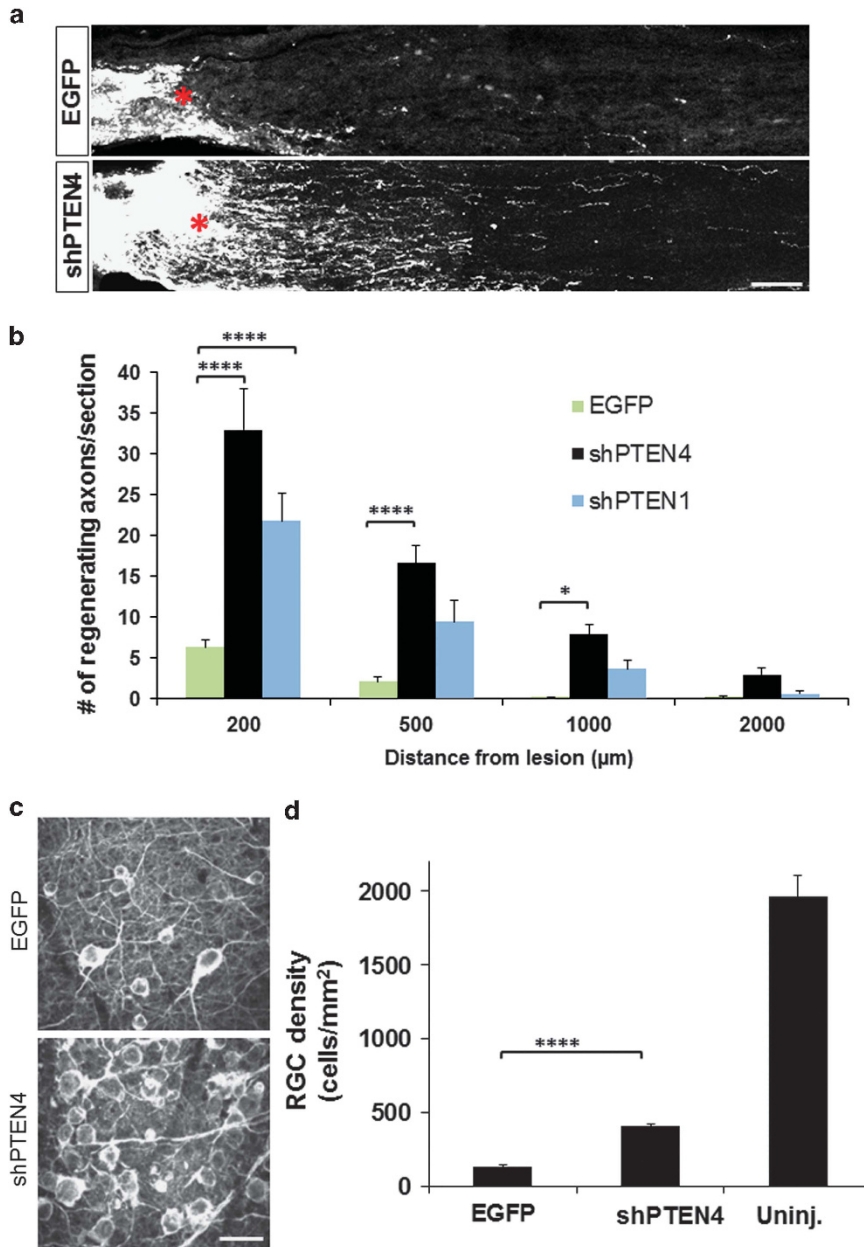


**Figure 2.** Assessment of RGC axon regeneration following AAV-shRNA-mediated knockdown of PTEN. **(a)** Representative optic nerve sections of mice receiving AAV2-shPTEN4 or control AAV2-EGFP injection. Red asterisk, lesion site. **(b)** Quantification of regenerating axons in control and shPTEN-treated animals ( $n=5$ /group) at different distances from the lesion site. The data are represented as mean number of axons per section. **(c)** Representative images of TUJ1-stained wholemount retinae for both groups. **(d)** Quantification of RGC density ( $n=5$ /group). Error bars, s.e.m.; \*\*\*\* $p < 0.0001$ ; \*\*\* $p < 0.001$ , \* $p < 0.05$  analysis of variance with Bonferroni correction **(b)** and Student's unpaired *t*-test **(d)**. Scale bars, 100  $\mu$ m **(a)**; 20  $\mu$ m **(b)**.



increase in survival is similar to that seen in the PTEN KO mice.<sup>1</sup> Overall, these data demonstrate that PTEN knockdown, albeit at a lower level than the PTEN KO mice, increases RGC axon regeneration in adult mice.

#### Assessment of combinatorial AAV and RNAi strategy to enhance long-distance axon regeneration

PTEN is one of many factors known to regulate RGC axon regeneration. Other strategies that were shown to facilitate long-distance RGC axon regeneration include deletion of SOCS3 or Klf4, and elevation of CNTF.<sup>2,12–18</sup> Given the synergistic effects induced by combining PTEN KO mice with modulation of the CNTF/signal transducer and activator of transcription-3 pathway, we sought to test combining RNAi and AAV approach to target these factors and further improve regeneration. First, we generated AAV

expressing shRNA against SOCS3 using the SIBR vector system, but this failed to drastically knockdown SOCS3 expression (data not shown). Given that elevation of CNTF using AAV vector allows significant increase in long-distance regeneration in the injured optic nerve,<sup>12–15,19</sup> we then tested combining AAV-CNTF with AAV-shPTEN. To mimic clinical situations, all animals in subsequent experiments received intravitreal injection immediately after an optic nerve crush. Consistent with the previous studies, we observed that animals receiving the AAV expressing a secretable form of CNTF alone show significant increase in regeneration (Figures 3a and b). Double combination of AAV-shPTEN with AAV-CNTF did not result in a significant increase compared with AAV-CNTF alone (Figures 3a and b). Next, we tested the effect of biweekly application of cell permeant cAMP analog, cpt-cAMP, in improving axon regeneration in the

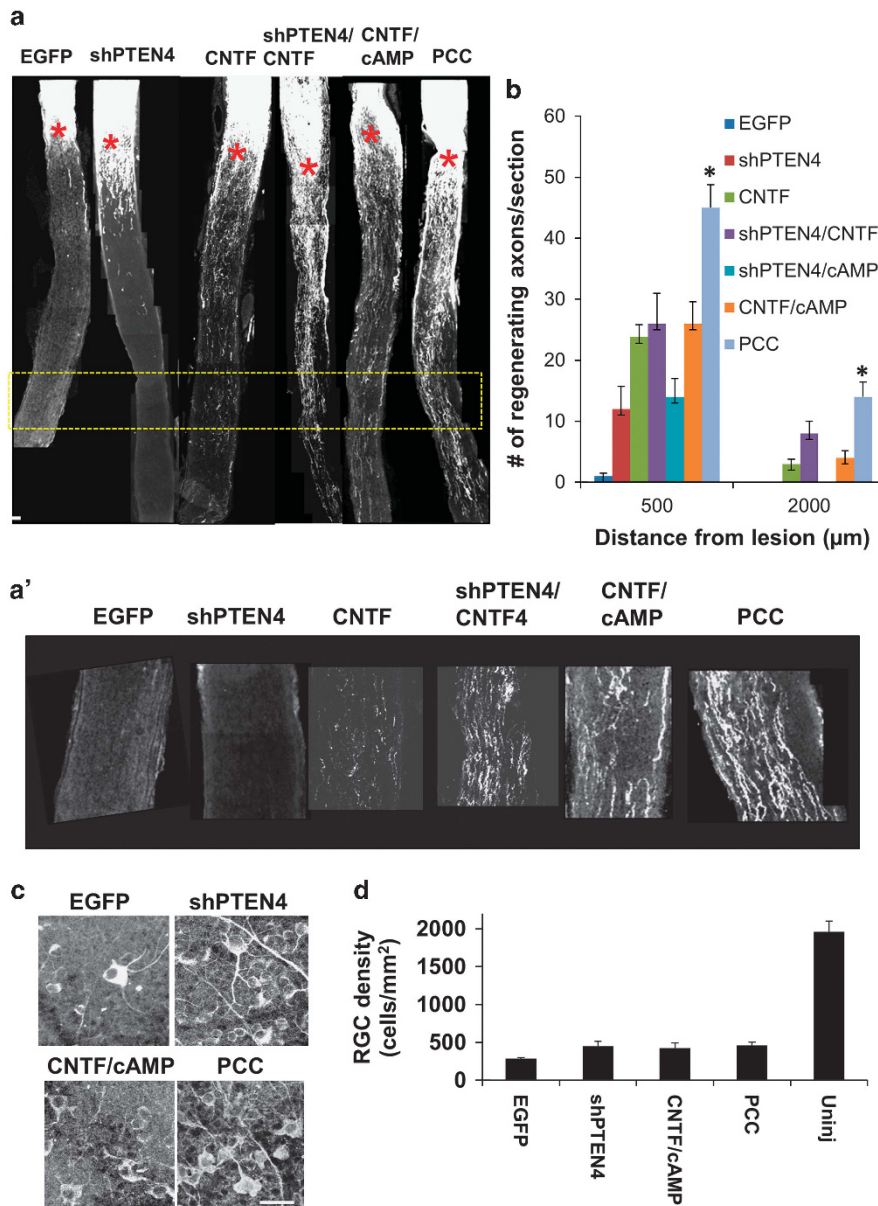


**Figure 3.** AAV-shPTEN, AAV-CNTF and cpt-cAMP further improves lengthy RGC axon regeneration. **(a)** Representative optic nerve sections of mice receiving various AAV treatments. Control, AAV2-EGFP; shPTEN4, AAV2-shPTEN4; CNTF, AAV-CNTF; CNTF/cAMP, AAV2-CNTF/cpt-cAMP; PCC, AAV2-shPTEN4/AAV2-CNTF/cpt-cAMP. Red asterisk, lesion site. **(a')** Higher-magnification images of the boxed area in **(a)**. **(b)** Quantification of regenerating axons at different distances from the lesion site ( $n = 6–8$ /group). \* $P < 0.05$ , Bonferroni test (PCC significantly different to AAV-CNTF and AAV-CNTF/cpt-cAMP groups). **(c)** Representative images of TUJ1-stained wholemount retinæ from mice receiving various AAV treatments. **(d)** Quantification of RGC density ( $n = 6$ /group). Error bars, s.e.m.. Scale bars, 100 μm **(a)**; 20 μm **(d)**. Uninj, uninjured.

background of AAV-shPTEN and AAV-CNTF. Previous studies have shown that cpt-cAMP can facilitate central nervous system axon regeneration by recruiting multiple mechanisms including down-regulation of SOCS3 as well as activating mitogen-activated protein kinase and protein kinase A pathways.<sup>17,20</sup> Indeed, this three-way combination of AAV-shPTEN4, AAV-CNTF and cpt-cAMP (hereafter referred as 'PCC' treatment) led to a marked increase in the number of regenerating axons; there is more than threefold increase in the number of axons regenerating up to 2 mm distal to the lesion compared with AAV-CNTF alone (Figures 3a and b;  $n=6-8$  per group). Of note, double combination of shPTEN and cpt-cAMP does not result in an obvious increase in axon regeneration compared with shPTEN treatment alone (Figure 3b). We also assessed RGC survival rates in the combinatorial paradigm using TUJ1 immunostaining, and observed that mice receiving PCC treatment have similar RGC survival (that is, over 20% survival compared with the contralateral uninjured retina) compared with AAV-shPTEN4 and AAV-CNTF/cpt-cAMP-treated groups in this post-injury treatment paradigm (Figures 3c and d). Overall, these results show that concomitant modulation of PTEN, CNTF and cAMP using a combination of viral, RNAi and pharmacotherapy approaches greatly enhances long-distance axon regeneration.

#### Assessment of RGC axon regeneration in PCC-treated mouse brains

Next, we examined the extent to which the regenerate RGC axons in PCC-treated animals extend beyond the optic chiasm and reach their visual targets. To this end, we used tissue clearing and light sheet fluorescence microscopy (LSFM) to image regenerating axons in whole mouse optic nerves and brains without the data loss that results from tissue sectioning.<sup>21,22</sup> This protocol uses tetrahydrofuran (THF) and a mixture of benzyl alcohol and benzyl benzoate to turn optic nerves and brains relatively transparent (Figure 4a), allowing visualization of the entire optic projection in whole tissues (Figure 4b). Animals received crush injury followed immediately by PCC treatment or AAV-EGFP injection. By 4–6 weeks post injury, regenerating axons reach the optic chiasm. About 20% of these axons extend into the opposite, uninjured optic nerve (Figures 4c–e). Similar or higher numbers of regenerating axons are found in the ipsilateral compared with the contralateral optic tract (Figures 4c and e) en route to more distal visual targets. Similar to the previous studies,<sup>14,22,23</sup> at 10–14 weeks post injury ( $n=13$ ), path-finding errors are evident in the brain as most axons extend dorsally, parallel to the third ventricle and do not find the distant brain targets (that is, superior colliculus and lateral geniculate nucleus; data not shown).

#### Characterizing individual axons' morphologies in a visual target

Importantly, regenerating axons are found in and around RGCs' first brain target the suprachiasmatic nucleus (SCN), located directly above the optic chiasm (Figure 5a). In control animals treated with AAV-EGFP ( $n=14$ ), we do not detect any CTB-labeled axons in the brain (Figure 5b). The growing tips of elongating axons sense their post-synaptic partners within the target to begin to form arbors and to establish synaptic connection. Do the adult RGC axons regenerating long distances through the optic nerve have the ability to sense their target and arborize? Traditionally, morphological analysis of axon terminals and arborization is carried out in histological sections. However, tissue sections provide limited spatial information, making it difficult to determine unequivocally whether the axon terminals are in fact located within a correct region. It is also difficult to ascertain the extent of arborization, a key step toward establishing a proper target reconnection. Here, we sought to expand the application of whole-tissue imaging techniques and to evaluate qualitatively the growth behavior as axons reach a correct visual target, the SCN.

To this end, we scanned individual 2D LSFM images of mouse brains to visualize CTB-labeled axons. We took advantage of the fact that the number of axons that reach the SCN is small (ranging between 5 and 40 axons per animal), allowing us to visualize, trace and sample single axons and their entire arbors. The vast majority of PCC-treated animals (11 out of 13 mice) had regenerating axons in the SCN. Figure 5 shows examples of two different animals with regenerating RGC axons reaching the SCN (Figures 5c and d). We were able to trace all visibly distinct axons in 2D optical slices and then compile these slices into a 3D reconstruction (Figures 5e–j). In total, we traced 18 axons that reach the SCN. Overall, we observe at least four different re-growth patterns in and around the SCN. First, some axons approach the SCN but turn and bypass the region. Figure 5e shows an example of such behavior where an axon bifurcates outside the SCN and its branches extend and wrap around the SCN, suggesting that these axons may be repelled and actively prevented from entering this nucleus. Second, some axons enter the SCN, but they traverse and their terminals are found outside the region (Figure 5f). In this category, axons often branch within the SCN but the arbors exit and continue to extend outside the SCN (Figure 5g). Thus, these axons appear to lack signals that facilitate target recognition. Third, terminals of some axons are found inside the SCN (Figure 5h). Fourth, there are axons that generate complex arbors within the target (Figures 5i and j). Figure 5i shows tracing of such fiber entering the SCN and generating complex arbors. Immediately after entering the contralateral SCN, this axon bifurcates and its branches subsequently generate multiple arbors. The branches stemming from this individual axon extend and cover a large field area within the SCN, suggesting the possibility that they may have made synapses with multiple SCN neurons.

#### Synaptogenesis

To find evidence of re-synaptogenesis by regenerated axons, we performed immunohistochemistry using an antibody against vesicular glutamate transporter 2 (Vglut2), a major presynaptic protein of RGCs. We observe that some CTB-labeled axons in the SCN (the anatomical location depicted in Figure 6a) have Vglut2-positive patches at bouton-like structures and along the axonal length (Figure 6b), suggesting an accumulation of the molecular machinery characteristic of a presynaptic terminal. To further confirm the ability of regenerating axons to make reconnection with the target neurons, we used the trans-synaptic reporter mouse line, *iZ/WAP*.<sup>24</sup> These transgenic mice express a Cre recombinase-inducible wheat germ agglutinin (WGA) under the control of the CMV, cytomegalovirus, promoter. Cre excision is indicated by WGA expression, and WGA acts as a trans-synaptic tracer, allowing identification of the synaptic contacts of Cre-expressing neurons.<sup>24</sup> In normal animals, between 40 and 80% of RGCs expressed WGA at 2 weeks following intravitreal AAV serotype-2 (AAV2)-Cre injection as shown by immunohistochemistry (Figure 6c). In accordance, many WGA<sup>+</sup> cells (that is, cells that are post-synaptically connected with RGCs) are visible in the SCN of uninjured animals (Figure 6d). Similarly, WGA<sup>+</sup> cells are present in the lateral geniculate nucleus in uninjured animals (Figure 6e). In contrast, no WGA<sup>+</sup> cells are detected in injured animals receiving control AAV2-EGFP injection ( $n=5$ ; Figure 6f). In some PCC animals (3 out of 10 animals), we observe WGA<sup>+</sup> cells in the SCN in close proximity to CTB<sup>+</sup> axons, indicating that these regenerate RGCs reform synapses with the target (Figures 6g and h). Overall, these data suggest that following the combinatorial treatment, individual regenerating axons possess varying capacity to recognize the target, and are able to form synapses and reconnect with the target neurons.

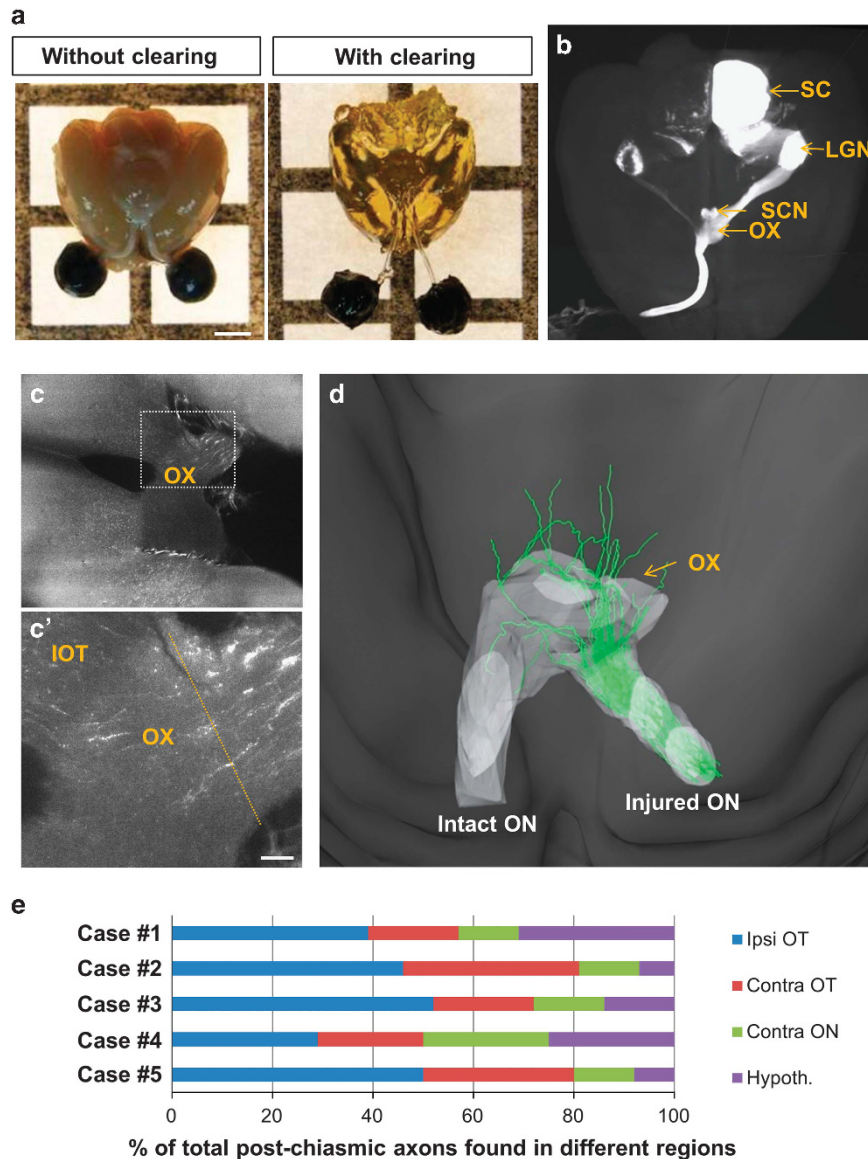


**Figure 4.** Tissue clearing and ultramicroscopic assessment of axonal trajectories in the optic chiasm of PCC animals. **(a)** Adult mouse brains with and without tissue clearing. The eyes and optic nerves are attached to the brain. **(b)** Top view of an intact mouse brain. Brain from an uninjured mouse shows the entire trajectory of CTB-labeled RGC axons: all visual targets are visible, including the suprachiasmatic nucleus, lateral geniculate nucleus, and superior colliculus, ipsi- and contralaterally to the injected eye. **(c)** A horizontal optical slice from an unsectioned brain of a PCC-treated animal shows CTB-labeled axons in the optic chiasm. **(c')** Higher-magnification of the boxed area in **(c)**. **(d)** Reconstruction of traced axons through the chiasm. **(e)** Quantification of axonal trajectories into different regions in five different cases (that is, ipsi- and contralateral optic tracts, contralateral optic nerve and hypothalamic regions). Contra, contralateral; Hypothal. Hypothalamic region; Ipsi, ipsilateral; IOT, ipsilateral optic tract; LGN, lateral geniculate nucleus; ON, optic nerve; OT, optic tract; OX, optic chiasm; 3rd V, 3rd ventricle; SC, superior colliculus; SCN, suprachiasmatic nucleus. Scale bars, 100  $\mu$ m.

## DISCUSSION

Previous studies have demonstrated that RGCs induced to regenerate in PTEN KO mice travel the entire length of the optic nerve<sup>1</sup> or, in combination with other factors, reach the targets<sup>3,25</sup> and induce partial recovery of visual functions.<sup>4</sup> Although these KO mouse studies have revealed some key molecular mechanisms underlying axon regeneration, it remained to be seen whether a non-transgenic approach that targets PTEN alone or in combination can also promote a similar degree of optic nerve regeneration and target re-innervation. As axonal damage in the optic nerve causes irreversible loss of visual functions in glaucoma and after trauma, therapeutically relevant strategies that promote

regeneration through the optic nerve and reconnection have important clinical implications. More broadly, therapeutic strategies designed to improve RGC axon regeneration may provide ideas to treat injuries in other long central nervous system tracts including the spinal cord.

Previous studies have reported successful uses of non-transgenic PTEN blockers to promote axon regeneration after nerve injury. Following a spinal cord injury, PTEN antagonist peptide or AAV-shPTEN were shown to improve axon regeneration in the spinal cord.<sup>9,26,27</sup> Others have demonstrated that PTEN inhibitor bisperoxovanadium enhances regeneration of sensory axons.<sup>28</sup> However, it has not been established whether



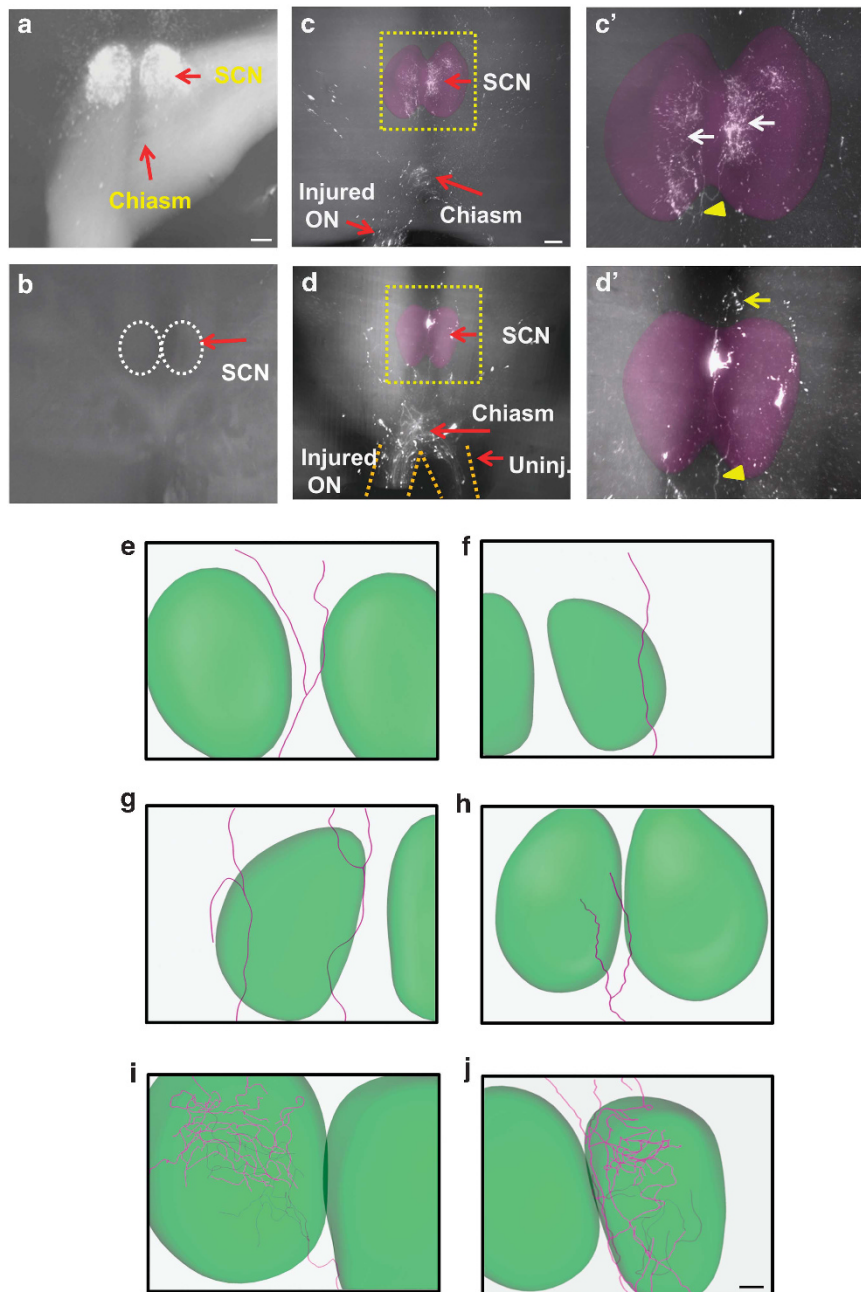


**Figure 5.** Ultramicroscopic visualization of axonal projections in mouse visual target. **(a)** Optic chiasm, optic tract and SCN shown by CTB labeling in a cleared, uninjured brain. **(b)** Bottom view of a brain containing the SCN (that is, dotted circles) imaged from a brain of an injured control mouse subjected to AAV-EGFP injection. None of the control animals had regenerating axons in the brain. **(c)** and **(d)** Bottom view of brains of two different PCC-treated animals showing regenerated axons in the chiasm and SCN. Yellow arrowhead indicates a regenerating axon extending into the SCN. Yellow arrow indicates distal end of the same axon showing continued growth beyond the SCN. White arrows in **c** indicate extensive arborization. **(c')** and **(d')** High magnification of the boxed areas in **c** and **d**. **(e–j)** Reconstructions of single axons showing various growth patterns. In **e**, an axon bypasses the target. In **f** and **g**, axons traverse the target. In **h**, axon terminals are found within the SCN. In **i** and **j**, axons enter the SCN and form complex arborization. ON, optic nerve; Uninj, uninjured; SCN, suprachiasmatic nucleus. Scale bars, 100  $\mu\text{m}$ .

AAV-shRNA that suppresses PTEN would induce regeneration in RGC axons. More importantly, whether combining RNAi knockdown of PTEN with other non-transgenic strategies known to increase neuron's growth ability could further enhance long-distance axon regeneration has not been directly addressed.

Here we compare rates of RGC axon regeneration following PTEN knockdown using two AAV vectors each carrying different PTEN target sequences. Despite protein knockdown efficacy as high as 70–90%, the effect on axon regeneration is far less robust

than that seen after PTEN deletion in transgenic mice. This difference could be attributed to potential off-target effects associated with RNAi (that is, silencing of pro-regenerative genes); however, this is unlikely as the two AAV-shPTEN vectors target different sequences within PTEN. Furthermore, the shPTEN1 used in this study was previously shown to cause no detectable off-target effects when the closest potential off-target genes were examined.<sup>10</sup> Thus, it is more likely that the weaker regeneration seen with RNAi is due to incomplete PTEN silencing, a common

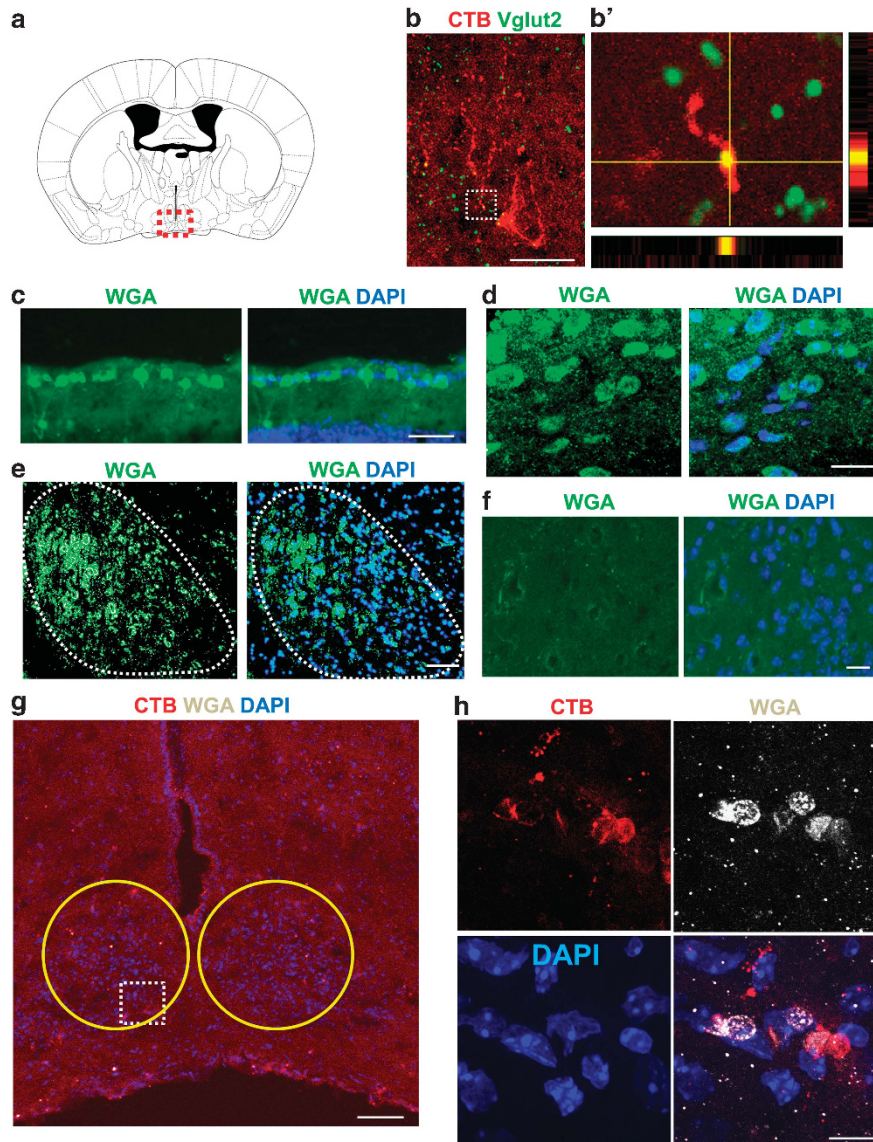


**Figure 6.** Regenerate axons following PCC treatment form synapses in the SCN. **(a)** Schematic coronal brain section showing the SCN marked in a dotted red rectangle. **(b)** CTB-labeled axons (red) in the SCN express presynaptic marker Vglut2 (green). **(b')** High-magnifications of the boxed area in **b**, with XZ and YZ projections at the yellow crosshairs. **(c)** Retinal cross-section showing RGCs expressing WGA (green) 6 weeks following AAV-Cre injection in iZ/WAP mice. 4'-6-Diamidino-2-phenylindole (DAPI; blue) is used in these tissue sections for nuclear staining. **(d)** WGA<sup>+</sup> cells in the SCN of an uninjured animal. WGA (green) and DAPI (blue). **(e)** WGA<sup>+</sup> cells in the LGN (as marked by dotted line) of an uninjured animal. WGA (green) and DAPI (blue). **(f)** No WGA<sup>+</sup> cells are detected in the injured AAV-EGFP control mice ( $n=5$ ). **(g)** Low-magnification coronal brain section showing the SCN of an injured PCC animal, marked in a yellow circles immunostained with antibodies against WGA. CTB, red; DAPI, blue. **(h)** High magnification of the dotted area in **g** showing CTB<sup>+</sup> axons (red) wrapping or making close contact with WGA<sup>+</sup> cells in the SCN. Scale bars, 50  $\mu\text{m}$ .

limitation in the use of shRNA technology.<sup>29</sup> In many instances, a low level of residual expression may still be sufficient for gene function. For example, conditional PTEN heterozygote mice typically display less severe phenotypes than null-homozygotes.<sup>30</sup> In accordance, we observe no obvious increase in axon regeneration after heterozygous PTEN ablation (that is, PTEN<sup>f/+</sup> mice subjected to intravitreal AAV-Cre injection; data not shown).

Virally expressed CNTF represents a potent way to induce long-distance RGC axon regeneration. Consistent with the previous studies,<sup>12–15,19</sup> AAV-CNTF alone results in a significant induction of long-distance regeneration, and cAMP analog did not significantly enhance axon regeneration in the background of AAV-CNTF.<sup>20,31</sup> However, combined treatment of cAMP analog, AAV-shPTEN and AAV-CNTF greatly enhanced regeneration and allowed more

axons to reach the brain. Interestingly, similar enhancement in regeneration has been reported when PTEN depletion and cAMP analog are combined with zymosan.<sup>25</sup> Mechanistically, previous studies have demonstrated that axon regeneration induced by PTEN depletion relies on downstream activation of Akt/mammalian target of rapamycin. On the other hand, axon regeneration induced by SOCS3 deletion or CNTF elevation is dependent on activation of the signal transducer and activator of transcription-3 pathway.<sup>1–3</sup> Multiple signaling pathways and molecules have been suggested to mediate the pro-regenerative effect of cAMP, including activation of mitogen-activated protein kinase, protein kinase A and cAMP response element-binding protein.<sup>17,20,32</sup> It has also been shown that cAMP can reduce CNTF-induced SOCS3 expression, diminishing the effect of this negative feedback



system.<sup>33</sup> Thus, it is likely that PCC treatment activates multiple pathways and mounts complementary growth programs that ultimately lead to more robust regeneration. However, the intricate mechanisms underlying the crosstalk between these molecules are unknown and await future elucidation.

Although mammalian RGCs can be induced to regenerate along the optic nerve, axons fail to correctly pathfind to their distant targets, the lateral geniculate nucleus and superior colliculus. These observations are consistent with the notion that axons do not simply re-use degenerating optic tracts.<sup>34</sup> Nonetheless, some regenerating axons successfully reach a target that is located much closer to the eye, the SCN. Using whole-tissue imaging, we provide single-fiber projection data that unequivocally reveal the behaviors of regenerating RGC axons as they reach this target. During development, growing RGC axons navigate towards their targets where they arborize and form synapses.<sup>7,35,36</sup> The transition from axon extension to target recognition and axon branch initiation is regulated by spatiotemporal expression of receptors and respective ligands in the axons and target regions. In particular, local expression of growth factors such as brain-derived neurotrophic factor (BDNF) and fibroblast growth factor 2 (FGF2) have been shown to have critical roles in modulating axon arborization and synaptic formation in the visual targets.<sup>6,36,37</sup> Do adult mammalian brains express relevant target cues, and do the regenerate RGC axons retain the capacity to recognize correct targets? These questions have been addressed extensively using peripheral nerve graft experiments, in which transected RGC axons are permitted to regenerate through a segment of peripheral nerve and reinnervate their targets.<sup>38–44</sup> These studies have indicated the presence of considerable axon arborization and synaptic connection in the SC and concluded that both optic axons and target neurons in adult mammals retain recognition ability.

In this study, use of single fiber tracing decisively shows extensive axon arborization, thereby providing morphological evidence of some axons' ability to recognize and reconnect with a visual target, whereas other axons seem to be repelled from entering this site. Of note, we observed the presence of synaptic marker (that is, Vglut2) in a variety of cases that include animals with relatively high number of axons in the SCN as well as animals with relatively low axon numbers. Thus, it is likely that regenerated axons with or without extensive arborization may make synapses in the SCN. This is further supported in trans-synaptic reporter mouse line, in which WGA-labeled cells were observed in SCN, indicating that the axons indeed made connection with the target. Recently, it was reported that axons of *pten/socs3* KO animals make synaptic connections with SCN neurons following pre-chiasmatic lesion.<sup>45</sup> However, it is not established whether the PCC in this study or the *pten/socs3* KO allows restoration of visual functions. Our laboratory is currently investigating this question. As the SCN is normally innervated by a small population intrinsically photosensitive RGCs, a question rises as to whether there is any degree of neuron-target selectivity in adult animals. Although several studies have used single-cell labeling to characterize axon targeting and branching patterns of different RGC types in lower species such as zebrafish and *Drosophila*,<sup>7,37</sup> no such comprehensive data currently exist for mammals. In this regard, it will be very interesting in the future to define normal targeting and arborization patterns of individual RGC types and assess the degree to which regenerating axons recapitulate this process. In light of different transgenic mouse lines in which distinct RGC subtypes including intrinsically photosensitive RGCs are labeled, initiation of such analysis may be feasible.<sup>35,46</sup>

In summary, our data highlight the limitation of shRNA technology in fully mimicking KO regeneration phenotypes, and indicate that combining AAV, shRNA and pharmacotherapy represents an alternative and effective strategy to improve axon regeneration, and importantly, target reconnection in wild-type

animals. Further, extended application of whole brain imaging underscores technical improvement in conducting a systematic evaluation of axon targeting and uncovers heterogeneous and distinct terminal patterns by the individual regenerating axons.

## MATERIALS AND METHODS

### Cloning and generation of AAV2-shPTEN, AAV2-Cre and AAV2-CNTF

To suppress PTEN expression, we adopted a shRNA strategy, based on SIBR vectors,<sup>8</sup> in which shRNA is located in an intron and flanked by sequences derived from mir155, an endogenous intronic shRNA. To maximize the probability of effectively targeting PTEN, four separate shRNA sequences, each targeting a different region of PTEN were concatenated in a single plasmid, which was then used to produce AAV (AAV-shPTEN). Four sequences that target both mouse and rat PTEN were designed using siDIRECT website and design rules:<sup>47</sup> four targeted sequences for PTEN are: 5'-GCAGAAACAAAAGGAGATATCA-3'; 5'-GATGATGTTTGAAACTATTCCA-3'; 5'-GTAGAGTCTCCACAACAGA-3'; 5'-GATGAAGATCAGCATTACAAA-3'. Oligonucleotides encoding hairpin loops that included these sequences and deliberate mis-matches in the non-target strand were synthesized, annealed, inserted into the SIBR knockdown vector, and concatenated into a single plasmid as described.<sup>8</sup> A region of the SIBR knockdown vector comprising the ubiquitin promoter, intronic sequences, knockdown cassette and EGFP open reading frame was cloned into an AAV-compatible plasmid (AAV-multiple cloning site (MCS), Stratagene, La Jolla, CA, USA), from which the CMV promoter, intron and MCS were removed. SIBR anti-luciferase control shRNA was transferred to AAV plasmid similarly. To construct AAV expressing a secretable form of CNTF, an AAV-compatible SIBR vector was created by PCR-amplifying the knockdown cassette of a SIBR vector with primers that created 5' MluI (5'-ACGCGTTAAACTGGCTCCGCGCC-3') and 3' ClaI (5'-ccgcccGATCGATTCACTTGATCA GCTCGTCCA-3') sites. This cassette was inserted into a Stratagene AAV plasmid, replacing the CMV promoter and B-globin intron. The resulting AAV-SIBR plasmid was then modified via bridge PCR to create *KpnI* and *BglII* sites to flank the EGFP open reading frame. Plasmid DNA encoding human CNTF was purchased from OpenBiosystems (Accession: BC068030) and the open reading frame was amplified using a forward primer that incorporated both a 5' *KpnI* restriction site and the NGF signal peptide sequence (5'-GGTACCATGTCCATGTTGTTCTACACTCTGATCACAGCTTTTCTGATC;GGCATAACAGGCGGCTTTCACAGAGCATTACCGC-3') and a reverse primer that incorporated 3' *BglII* site (5'-AGATCTCTACATTTCTTGTTGTTAGCAA-3'). PCR-amplified CNTF was then used to replace the EGFP ORF in the AAV-SIBR vector via standard restriction digest and ligation. All enzymes were purchased from New England Biolabs (Ipswich, MA, USA). Plasmids were then used to produce AAV2 (1–4 × 10<sup>13</sup> particles per ml) at the University of Miami Viral Vector Core. For making AAV2 expressing Cre recombinase, the cDNA of Cre was inserted downstream of the CMV promoter/β-globin intron enhancer in the plasmid pAAV-MCS (Stratagene), containing the AAV2 inverted terminal repeats and a human growth hormone polyA signal. pAAV-RC (Stratagene) that encodes the AAV2 genes (rep and cap) and the helper plasmid (Stratagene) that encodes E2A, E4 and VA were used for co-transfection in 293T cells to generate recombinant AAV. Plasmids were then used to produce AAV2 (1–4 × 10<sup>13</sup> particles per ml) at the University of Miami Viral Vector Core.

### Animals

All animal procedures were performed with the approval of the Institutional Animal Care and Use Committee (IACUC) at University of Miami. C57BL/6 (male or female; Charles River Laboratory, Wilmington, MA, USA) mice were used in this study, except for the WGA experiment in Figure 6 in which iZ/WAP mice (B6;129-Tg(CMV-Bgeo,-WGA,-ALPP)1Mgmj/J, Jackson Laboratory, Bar Harbor, ME, USA; Stock number, 017524)<sup>24</sup> were used. The age of animals used at the start of each experiment was between 4 and 6 weeks. Animals were randomly assigned to different treatment groups. The investigator who analyzed the data was not blinded to the animal identity. The numbers of animals (*n*/group) used for each experiment range from 3 up to 14 depending on the type of experiment and are listed in the figure legends.

### Intraorbital optic nerve crush

The optic nerve was exposed intraorbitally and crushed with jeweler's forceps (Dumont #5; Roboz, Gaithersburg, MD, USA) for 10 s ~1 mm behind the optic disc. To preserve the retinal blood supply, care was taken not to damage the underlying ophthalmic artery. After the surgical procedure, mice received a subcutaneous injection of buprenorphine (0.05 mg kg<sup>-1</sup>, Bedford Lab, Bedford, OH, USA) as post-operative analgesic. Eye ointment containing atropine sulfate was applied preoperatively to protect the cornea during surgery.

### Intravitreal injection

For each intravitreal injection, a glass micropipette was inserted into the temporal eye posterior to the ora serrata and deliberately angled to avoid lens damage. Approximately 2  $\mu$ l of vitreal fluid were withdrawn before injection to accommodate the same volume of either virus mix or CTB conjugated with Alexa 555 (Invitrogen, Waltham, MA, USA). AAV was administered either 2 weeks before or immediately after crush. cpt-cAMP (8-(4-chlorophenylthio) adenosine-3',5'-cyclic monophosphorothioate; Sigma-Aldrich (St Louis, MO, USA); 50  $\mu$ M) was injected intravitreally on the day of crush and biweekly (that is, every other week) thereafter until euthanasia.<sup>25</sup> CTB (2  $\mu$ g  $\mu$ l<sup>-1</sup>) was injected 2–4 days before euthanasia. To visualize RGC projection in normal mice, CTB was injected and animals were euthanized 2–4 days later. After the completion of eye injection, animals received the same post-operative treatment as described above.

### Immunohistochemistry/immunocytochemistry

Animals were perfused transcardially with phosphate-buffered saline (PBS) followed by 4% paraformaldehyde (PFA) in PBS, then tissues dissected and post-fixed with 4% PFA in PBS for 1 h at room temperature. For histological sectioning, samples were cryoprotected by incubating in 30% sucrose in PBS for 48 h. Optic nerves and retinae were cryosectioned to 10 and 20  $\mu$ m thickness, respectively. Tissue sections were blocked in 5% normal goat serum and 0.3% Triton X-100 in PBS for 1 h and incubated with primary antibodies diluted in blocking buffer overnight at 4 °C, followed by 1 h incubation with secondary antibodies at room temperature. For cortical neuron immunocytochemistry, cells were fixed for 15 min in 4% PFA, washed with PBS and stained as described above. Primary antibodies used were anti- $\beta$ III-tubulin (1:800; Covance, Princeton, NJ, USA; #PRB-435P), PTEN (1:200; Cell Signaling Technology (CST), Danvers, MA, USA; #9559S), vesicular glutamate transporter 2 (Vglut2; 1:500; Synaptic Systems, Goettingen, Germany; #135304), WGA lectin (1:100; Sigma-Aldrich; #T4144-1VL) and GFP (1:1,000; Abcam, Cambridge, MA, USA; #ab13970). All secondary antibodies (used at dilution of 1:400; Cy2, Cy3 or Cy5) were purchased from Jackson ImmunoResearch (West Grove, PA, USA).

### Measurement of PTEN immunoreactivity

The mean PTEN staining intensity in RGCs was measured using ImageJ software (National Institute of Health, Bethesda, MD, USA). Values for PTEN were based on eight cells per section, two sections per case and three per groups. Only GFP<sup>+</sup> cells in the ganglion cell layer with visible axon projection (that is, RGCs) were selected for measurement. As negative controls, we omitted the primary antibody. Individual mean values were corrected by staining levels in the corresponding negative controls (that is, background subtracted) and then averaged across each group.

### Cortical cell culture

Mixed cortical cultures from P2 rat pups were prepared as previously described.<sup>48</sup> Briefly, cells were dissociated by sequential digestion in papain (20 U ml<sup>-1</sup>, Worthington, Lakewood, NJ, USA) and trypsin (2.5%, Invitrogen), then cultured in supplemented Neurobasal media (Invitrogen) in 24-well Falcon plates on a substrate of poly-d-lysine, (100  $\mu$ g ml<sup>-1</sup>, Sigma-Aldrich) and laminin (100  $\mu$ g ml<sup>-1</sup>, Cultrex, Gaithersburg, MD, USA) at a density of 50 000 cells per well. AAV2-shPTEN or AAV2-anti-luciferase (4  $\times$  10<sup>8</sup> total particles) were applied. Cultures were maintained at 37 °C in a humidified CO<sub>2</sub> incubator for 6 additional days, with media exchanged every other day, then fixed in 4% PFA (Sigma-Aldrich)/4% sucrose (Sigma-Aldrich).

### Western blot

Cortical cells were lysed with RIPA buffer. The protein concentration of the supernatant was determined using the Bio-Rad (Hercules, CA, USA) protein assay reagent. Approximately 20  $\mu$ g of protein was loaded and separated in a 10% acrylamide-Bis solution (Bio-Rad) gel. The protein was transferred onto Hybond-C Super membrane (Amersham Biosciences, Little Chalfont, UK) and blocked with 5% skim milk in 0.1% Tween-20 in PBS. The

membranes were incubated with anti-PTEN (1:1000; CST; #9559 S) or anti- $\beta$ III tubulin (1:2000; Covance; #PRB-435 P) in 5% bovine serum albumin in Tween-20 in PBS overnight at 4 °C. The membranes were incubated in biotinylated secondary antibody at a 1:5000 dilution for 1 h at room temperature. The membranes were incubated with horseradish peroxidase-conjugated antibody (Jackson ImmunoResearch) before the labeled proteins were detected using the ECL agent (Pierce, Rockford, IL, USA), following the supplier's manual. The intensity of each band was quantified using the Image J. The relative level of PTEN was expressed as the ratio to  $\beta$ III-tubulin. The quantification was the average calculated from three biological replicates (that is, three independent cortical cell preparations).

### Cell survival and axon regeneration quantification

To quantify regenerating axons, the crush site was identified by tissue morphology and CTB signal intensity, and the number of CTB<sup>+</sup> axons that projected various distances from the lesion was recorded. At least four sections were counted for each animal. To quantify RGCs, the number of TUJ1<sup>+</sup> cells in the ganglion cell layer of at least four non-consecutive retina sections per animal was counted.

### Tissue clearing

Optic nerves and brains were prepared as described above and post-fixed overnight. Detailed description of tissue clearing is provided in our recent manuscripts.<sup>22</sup> Samples underwent dehydration by incubation in increasing concentrations of THF (Sigma-Aldrich) solutions. Optic nerves were incubated for 15 min each in 50% THF (diluted in water, v/v), 80% THF and 100% THF. Dehydrated optic nerves were rendered clear by incubating in a mixture of benzyl alcohol and benzyl benzoate (Sigma-Aldrich; at a ratio of 1:2) for 20 min. Adult mouse brains were gradually dehydrated with 50% THF for 12 h, 80% THF for 12 h and 100% THF for 3  $\times$  12 h, and cleared in a mixture of benzyl alcohol and benzyl benzoate for 12 h with constant shaking before imaging.

### LSFM and axon tracing

LSFM was performed as previously described.<sup>21,49</sup> For each optic nerve and brain, between 100 and 500 optical slices were imaged with LSFM (LaVision, Goettingen, Germany) at a scan speed of 0.5–1.5 s per slice. Images were collected at 2–5  $\mu$ m increments in the Z axis. Images, and 3D volume rendering, were prepared using Imaris software v7.6.1 (Bitplane, Zurich, Switzerland). CTB-labeled RGC axons in the brain were traced using Imaris Filament Tracer Module and SCN boundaries were marked with Imaris Surface Module. Axons were identified and manually traced in individual 2D optical slices (z stacks) and compiled to give a 3D reconstruction.

### Examination of trans-synaptic WGA labeling in iZ/WAP mice

Transgenic mice (B6;129-Tg(CMV-Bgeo-WGA-ALPP)1Mgmj/J, Jackson Laboratory; Stock number, 017524)<sup>24</sup> that express Cre recombinase-inducible WGA under the direction of the CMV promoter received optic nerve crush followed immediately by AAV-EGFP or PCC injection. One week following injury, AAV-Cre was injected intravitreally to induce WGA expression in RGCs. Five weeks after AAV-Cre injection, animals were perfused and tissues were collected for WGA immunohistochemistry.

### Statistics

Data were analyzed using analysis of variance and the Bonferroni within-groups comparison with additional testing using Dunnett's test or Student's *t*-test. Significant differences required *P* values < 0.05. Values were displayed as mean  $\pm$  standard error of mean (s.e.m.). Sample size (up to 14 per group) was chosen in accordance to several previous studies of optic nerve regeneration.<sup>1,4,18</sup>

### CONFLICT OF INTEREST

The authors declare no conflict of interest

### ACKNOWLEDGEMENTS

This work was supported by grants from US Army W81XWH-05-1-0061 (KKP), W81XWH-12-1-0319 (KKP), NEI 1R01EY022961-01 (KKP), Ziegler Foundation (KKP), Pew Charitable Trust (KKP), Craig H. Neilsen Foundation (KKP) and the Buoniconti Fund (KKP). We thank Imaging, and Viral Vector Core at the Miami Project to Cure Paralysis, Dr David Turner for SIBR vector, Dr Vance Lemmon and Dr John Bixby for guidance with shRNA vector, Drs William Hauswirth and Vince Chiodo for initial testing with AAV-CNTF, and Dr Bryan Luikart for shPTEN plasmid.

## REFERENCES

- 1 Park KK, Liu K, Hu Y, Smith PD, Wang C, Cai B *et al*. Promoting axon regeneration in the adult CNS by modulation of the PTEN/mTOR pathway. *Science* 2008; **322**: 963–966.
- 2 Smith PD, Sun F, Park KK, Cai B, Wang C, Kuwako K *et al*. SOCS3 deletion promotes optic nerve regeneration in vivo. *Neuron* 2009; **64**: 617–623.
- 3 Sun F, Park KK, Belin S, Wang D, Lu T, Chen G *et al*. Sustained axon regeneration induced by co-deletion of PTEN and SOCS3. *Nature* 2011; **480**: 372–375.
- 4 de Lima S, Koriyama Y, Kurimoto T, Oliveira JT, Yin Y, Li Y *et al*. Full-length axon regeneration in the adult mouse optic nerve and partial recovery of simple visual behaviors. *Proc Natl Acad Sci USA* 2012; **109**: 9149–9154.
- 5 Kotterman MA, Schaffer DV. Engineering adeno-associated viruses for clinical gene therapy. *Nat Rev Genet* 2014; **15**: 445–451.
- 6 Alsina B, Vu T, Cohen-Cory S. Visualizing synapse formation in arborizing optic axons in vivo: dynamics and modulation by BDNF. *Nat Neurosci* 2001; **4**: 1093–1101.
- 7 Robles E, Laurell E, Baier H. The retinal projectome reveals brain-area-specific visual representations generated by ganglion cell diversity. *Curr Biol* 2014; **24**: 2085–2096.
- 8 Chung KH, Hart CC, Al-Bassam S, Avery A, Taylor J, Patel PD *et al*. Polycistronic RNA polymerase II expression vectors for RNA interference based on BIC/miR-155. *Nucleic Acids Res* 2006; **34**: e53.
- 9 Zukor K, Belin S, Wang C, Keelan N, Wang X, He Z. Short hairpin RNA against PTEN enhances regenerative growth of corticospinal tract axons after spinal cord injury. *J Neurosci* 2013; **33**: 15350–15361.
- 10 Luikart BW, Schnell E, Washburn EK, Bensen AL, Tovar KR, Westbrook GL. Pten knockdown in vivo increases excitatory drive onto dentate granule cells. *J Neurosci* 2011; **31**: 4345–4354.
- 11 Hellstrom M, Harvey AR. Retinal ganglion cell gene therapy and visual system repair. *Curr Gene Ther* 2011; **11**: 116–131.
- 12 Leaver SG, Cui Q, Bernard O, Harvey AR. Cooperative effects of bcl-2 and AAV-mediated expression of CNTF on retinal ganglion cell survival and axonal regeneration in adult transgenic mice. *Eur J Neurosci* 2006; **24**: 3323–3332.
- 13 Leaver SG, Cui Q, Plant GW, Arulpragasam A, Hisheh S, Verhaagen J *et al*. AAV-mediated expression of CNTF promotes long-term survival and regeneration of adult rat retinal ganglion cells. *Gene Ther* 2006; **13**: 1328–1341.
- 14 Pernet V, Joly S, Dalkara D, Jordi N, Schwarz O, Christ F *et al*. Long-distance axonal regeneration induced by CNTF gene transfer is impaired by axonal misguidance in the injured adult optic nerve. *Neurobiol Dis* 2013; **51**: 202–213.
- 15 Pernet V, Joly S, Jordi N, Dalkara D, Guzik-Kornacka A, Flannery JG *et al*. Misguidance and modulation of axonal regeneration by Stat3 and Rho/ROCK signaling in the transparent optic nerve. *Cell Death Dis* 2013; **4**: e734.
- 16 Muller A, Hauk TG, Leibinger M, Marienfeld R, Fischer D. Exogenous CNTF stimulates axon regeneration of retinal ganglion cells partially via endogenous CNTF. *Mol Cell Neurosci* 2009; **41**: 233–246.
- 17 Park K, Luo JM, Hisheh S, Harvey AR, Cui Q. Cellular mechanisms associated with spontaneous and ciliary neurotrophic factor-cAMP-induced survival and axonal regeneration of adult retinal ganglion cells. *J Neurosci* 2004; **24**: 10806–10815.
- 18 Moore DL, Blackmore MG, Hu Y, Kaestner KH, Bixby JL, Lemmon VP *et al*. KLF family members regulate intrinsic axon regeneration ability. *Science* 2009; **326**: 298–301.
- 19 Hellstrom M, Pollett MA, Harvey AR. Post-injury delivery of rAAV2-CNTF combined with short-term pharmacotherapy is neuroprotective and promotes extensive axonal regeneration after optic nerve trauma. *J Neurotrauma* 2011; **28**: 2475–2483.
- 20 Hellstrom M, Harvey AR. Cyclic AMP and the regeneration of retinal ganglion cell axons. *Int J Biochem Cell Biol* 2014; **56**: 66–73.
- 21 Luo X, Yungher B, Park KK. Application of tissue clearing and light sheet fluorescence microscopy to assess optic nerve regeneration in unsectioned tissues. *Methods Mol Biol* 2014; **1162**: 209–217.
- 22 Luo X, Salgueiro Y, Beckerman SR, Lemmon VP, Tsoulfas P, Park KK. Three-dimensional evaluation of retinal ganglion cell axon regeneration and pathfinding in whole mouse tissue after injury. *Exp Neurol* 2013; **247**: 653–662.
- 23 Pernet V, Schwab ME. Lost in the jungle: new hurdles for optic nerve axon regeneration. *Trends Neurosci* 2014; **37**: 381–387.
- 24 Louis GW, Leininger GM, Rhodes CJ, Myers Jr MG. Direct innervation and modulation of orexin neurons by lateral hypothalamic LepRb neurons. *J Neurosci* 2010; **30**: 11278–11287.
- 25 Kurimoto T, Yin Y, Omura K, Gilbert HY, Kim D, Cen LP *et al*. Long-distance axon regeneration in the mature optic nerve: contributions of oncomodulin, cAMP, and pten gene deletion. *J Neurosci* 2010; **30**: 15654–15663.
- 26 Lewandowski G, Steward O. AAVshRNA-mediated suppression of PTEN in adult rats in combination with salmon fibrin administration enables regenerative growth of corticospinal axons and enhances recovery of voluntary motor function after cervical spinal cord injury. *J Neurosci* 2014; **34**: 9951–9962.
- 27 Ohtake Y, Park D, Abdul-Muneer PM, Li H, Xu B, Sharma K *et al*. The effect of systemic PTEN antagonist peptides on axon growth and functional recovery after spinal cord injury. *Biomaterials* 2014; **35**: 4610–4626.
- 28 Christie KJ, Webber CA, Martinez JA, Singh B, Zochodne DW. PTEN inhibition to facilitate intrinsic regenerative outgrowth of adult peripheral axons. *J Neurosci* 2010; **30**: 9306–9315.
- 29 Xu XM, Yoo MH, Carlson BA, Gladyshev VN, Hatfield DL. Simultaneous knockdown of the expression of two genes using multiple shRNAs and subsequent knock-in of their expression. *Nat Protoc* 2009; **4**: 1338–1348.
- 30 Fraser MM, Bayazitov IT, Zakharenko SS, Baker SJ. Phosphatase and tensin homolog, deleted on chromosome 10 deficiency in brain causes defects in synaptic structure, transmission and plasticity, and myelination abnormalities. *Neuroscience* 2008; **151**: 476–488.
- 31 Hellstrom M, Muhling J, Ehlert EM, Verhaagen J, Pollett MA, Hu Y *et al*. Negative impact of rAAV2 mediated expression of SOCS3 on the regeneration of adult retinal ganglion cell axons. *Mol Cell Neurosci* 2011; **46**: 507–515.
- 32 Gao Y, Deng K, Hou J, Bryson JB, Barco A, Nikulina E *et al*. Activated CREB is sufficient to overcome inhibitors in myelin and promote spinal axon regeneration in vivo. *Neuron* 2004; **44**: 609–621.
- 33 Park KK, Hu Y, Muhling J, Pollett MA, Dallimore EJ, Turnley AM *et al*. Cytokine-induced SOCS expression is inhibited by cAMP analogue: impact on regeneration in injured retina. *Mol Cell Neurosci* 2009; **41**: 313–324.
- 34 Wyatt C, Ebert A, Reimer MM, Rasband K, Hardy M, Chien CB *et al*. Analysis of the *astray/robo2* zebrafish mutant reveals that degenerating tracts do not provide strong guidance cues for regenerating optic axons. *J Neurosci* 2010; **30**: 13838–13849.
- 35 Osterhout JA, El-Danaf RN, Nguyen PL, Huberman AD. Birthdate and outgrowth timing predict cellular mechanisms of axon target matching in the developing visual pathway. *Cell Rep* 2014; **8**: 1006–1017.
- 36 McFarlane S, McNeill L, Holt CE. FGF signaling and target recognition in the developing *Xenopus* visual system. *Neuron* 1995; **15**: 1017–1028.
- 37 Cohen-Cory S, Fraser SE. Effects of brain-derived neurotrophic factor on optic axon branching and remodelling in vivo. *Nature* 1995; **378**: 192–196.
- 38 Aviles-Trigueros M, Sauve Y, Lund RD, Vidal-Sanz M. Selective innervation of retinorecipient brainstem nuclei by retinal ganglion cell axons regenerating through peripheral nerve grafts in adult rats. *J Neurosci* 2000; **20**: 361–374.
- 39 Vidal-Sanz M, Aviles-Trigueros M, Whiteley SJ, Sauve Y, Lund RD. Reinnervation of the pretectum in adult rats by regenerated retinal ganglion cell axons: anatomical and functional studies. *Prog Brain Res* 2002; **137**: 443–452.
- 40 Wizenmann A, Bahr M. Growth characteristics of ganglion cell axons in the developing and regenerating retino-tectal projection of the rat. *Cell Tissue Res* 1997; **290**: 395–403.
- 41 Sauve Y, Sawai H, Rasminsky M. Topological specificity in reinnervation of the superior colliculus by regenerated retinal ganglion cell axons in adult hamsters. *J Neurosci* 2001; **21**: 951–960.
- 42 Carter DA, Bray GM, Aguayo AJ. Regenerated retinal ganglion cell axons form normal numbers of boutons but fail to expand their arbors in the superior colliculus. *J Neurocytol* 1998; **27**: 187–196.
- 43 Sauve Y, Sawai H, Rasminsky M. Functional synaptic connections made by regenerated retinal ganglion cell axons in the superior colliculus of adult hamsters. *J Neurosci* 1995; **15**: 665–675.
- 44 Carter DA, Bray GM, Aguayo AJ. Regenerated retinal ganglion cell axons can form well-differentiated synapses in the superior colliculus of adult hamsters. *J Neurosci* 1989; **9**: 4042–4050.
- 45 Li S, He Q, Wang H, Tang X, Ho KW, Gao X *et al*. Injured adult retinal axons with Pten and Socs3 co-deletion reform active synapses with suprachiasmatic neurons. *Neurobiol Dis* 2014; **73C**: 366–376.
- 46 Hattar S, Kumar M, Park A, Tong P, Tung J, Yau KW *et al*. Central projections of melanopsin-expressing retinal ganglion cells in the mouse. *J Comp Neurol* 2006; **497**: 326–349.
- 47 Ui-Tei K, Naito Y, Takahashi F, Haraguchi T, Ohki-Hamazaki H, Juni A *et al*. Guidelines for the selection of highly effective siRNA sequences for mammalian and chick RNA interference. *Nucleic Acids Res* 2004; **32**: 936–948.
- 48 Blackmore MG, Wang Z, Lerch JK, Motti D, Zhang YP, Shields CB *et al*. Kruppel-like Factor 7 engineered for transcriptional activation promotes axon regeneration in the adult corticospinal tract. *Proc Natl Acad Sci USA* 2012; **109**: 7517–7522.
- 49 Erturk A, Mauch CP, Hellal F, Forstner F, Keck T, Becker K *et al*. Three-dimensional imaging of the unsectioned adult spinal cord to assess axon regeneration and glial responses after injury. *Nat Med* 2012; **18**: 166–171.